

## Contribution of entrainment and vertical plumes to the winter cascading of cold shelf waters in a deep lake

**Abstract**—Observations made from vertical moorings of thermistors and current meters are used to analyze the relative contribution of the entrainment of overlying water and the cold plumes convecting from the surface to the cascade of dense shelf waters down the sides of Lake Geneva. Assuming a steady state and ignoring the effects of the Earth's rotation, a simple model was introduced and 25 individual slugs of gravity currents were analyzed. The average drag coefficient, which includes the effects of friction on the slope and the interface between the gravity current and the ambient water, is found to be equal to  $C_D = (4.6 \pm 1.5) \times 10^{-3}$ . The volume flux in the gravity current increases with downslope distance—a consequence of both the entrainment of water into the gravity current and the supply of cold water from the plumes. Entrainment was found to be, on average,  $1.9 \pm 0.9$  times the contribution of vertical plumes, suggesting that the latter may be important in the dynamics of the cascade.

During periods in winter favoring convection, a relatively uniform heat loss from the water surface results in a spatial temperature variation where the temperature of the shallow well-mixed waters at the edges of deep lakes or that of continental shelves surrounding the oceans falls more rapidly than that of deeper waters overlying the thermocline. In consequence, water over shallow regions becomes relatively dense and descends the neighboring slope as a gravity current or “cascade.” Cascades are mechanisms for water exchange at the shelf edge (Huthnance 1995; Fer et al. 2001). In open waters far from the shore, dense surface waters sink, forming convective plumes (Killworth 1979; Marshall and Schott 1999). Provided that the thermocline is weak, both processes may cause deep mixing. Deep mixing events associated with winter cooling ventilate and oxygenate deep lake waters. McManus et al. (1996), for example, report oxygen budget studies of Crater Lake, Oregon, which yield a mean residence time of 2–4 yr for the deep water, which is partially mixed with surface waters each year. Deep mixing also imports nutrients, which are critical to primary productivity, into the euphotic zone (Crawford and Collier 1997).

There have been several observations of winter cascading in the ocean. Cooper and Vaux (1949) were the first to describe the phenomenon and presented evidence that Celtic Sea shelf waters cascaded down the continental slope. Tomczak (1985) and Hill et al. (1998) also provided detailed observations in the Bass Strait and the Malin Shelf, respectively. Recently, Fer et al. (2001) reported observations of winter cascading of cold shelf waters in Lake Geneva. There, the cascade is periodic on at least two time scales: a diurnal scale associated with gravity currents or ‘slugs’ of cold water lasting 8 h on average, and another of shorter period, typically 1–3 h, associated

with pulses of cold water traveling downslope through the gravity current in a manner similar to roll-waves in a steep open-channel flow.

The aim of this note is to provide estimates of the relative contributions of entrainment and of convective vertical plumes to the cascade down the sloping sides of Lake Geneva during these observations.

**Experiments**—Experiments were carried out in the vicinity of Buchillon (46°27'N, 6°32'E), on the northern shore of Lake Geneva. The bathymetry of the area was derived from repeated transects from shore. The mean slope values are 1° to 7 m depth, providing a relatively wide shallow-water shelf extending some 250 m from shore; a steep slope of 20° between 7 and 20 m; and 4.6° between 20 and 80 m depth. It is to this 20–80 m depth range that analysis is later applied. The lake is 310 m deep at its greatest depth. Measurements were made for 38 d from 30 December 1999 when the thermocline depth exceeded 55 m. Two vertical chains of self-contained temperature miniloggers deployed at depths of 21 and 55 m covered a vertical range at heights of 1.2–15 and 1.5–7.5 m above the bottom, respectively, and recorded at 2.5-min intervals to  $\pm 0.1^\circ\text{C}$  absolute accuracy with a resolution of  $0.015^\circ\text{C}$ . The vertical chains at 21 and 55 m depth consisted of 12 (1.2, 2.5, 4.5, 5, 5.5, 6.3, 7, 7.7, 8.5, 9.2, 11, 15 m above the bottom) and 8 (1.5, 3, 3.7, 4.5, 5.2, 6, 6.7, 7.5 m above the bottom) temperature miniloggers, respectively. The horizontal separation between the two lines is approximately 500 m. Currents were measured with Aanderaa RCM9-type current meters (referred to as ACM hereafter)—two deployed at 2 and 4 m above the bottom at 21 m depth and one at 2 m above the bottom at 55 m depth. The ACMs sampled every 5 min. An upward-looking RD Instruments workhorse broadband ADCP was installed at the bottom, close to the vertical chain at 55 m depth, profiling a vertical range from 5 to 50 m off the bottom, with 2-m bins. The system frequency of the ADCP is 300 kHz, and the continuous profile recording was averaged over 6-min intervals. Transects of CTD (conductivity, temperature, depth) profiles perpendicular to the shore were taken on several days throughout the observation period. The CTD sensors sample at 4.5 Hz, and the resolution of the temperature sensor was  $0.001^\circ\text{C}$ . The instrument lowering speed was  $\sim 10 \text{ cm s}^{-1}$ .

**The model**—The downslope movement in the gravity current and the physical processes involved are sketched in Fig. 1. The cold water near the slope is represented as a uniform layer of thickness,  $h$ , underlying an ambient deeper layer. The temperatures of the ambient water, the vertical plumes and the slug are  $\theta_{\text{amb}}$ ,  $\theta_p$ , and  $\theta$ , respec-

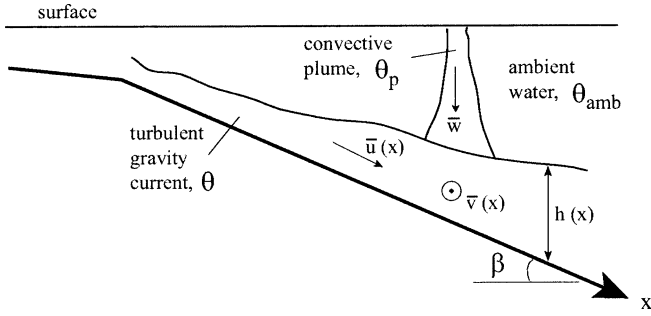


Fig. 1. Definition sketch of a turbulent gravity current adjacent to a sloping bottom. Symbols are defined in the text.

tively. Coordinate  $x$  is the distance in the downslope direction,  $\beta$  is the slope angle, and downslope and along-slope components of the mean flow are  $\bar{u}$  and  $\bar{v}$ , respectively. The mean vertical velocity of the plumes convecting from the surface is denoted by  $\bar{w}$ . For simplicity, we assume a steady state and ignore the effects of the Earth's rotation. The mean velocities inside the vertical plumes and the gravity current are assumed to be much greater than the velocities in the ambient water, and the downslope component of the mean plume velocity is negligible compared to the mean downslope flow (i.e.  $\bar{u} \gg \bar{w} \sin \beta$ ). The flow inside the gravity current is assumed to be fully developed and turbulent with high Reynolds numbers,  $Re$ . In the gravity current,  $Re$  is estimated to be  $\sim 3 \times 10^5$ . Following Turner (1973), we suppose that the turbulent motion in the gravity current and the shear across the interface between the gravity current and the ambient water lead to entrainment of water into the high turbulent region with a velocity  $E\bar{u}$ , where  $\bar{u}$  is the mean alongstream velocity and  $E$  is the proportionality constant or entrainment coefficient.

The volume flux in the gravity current increases with depth as a consequence of both the entrainment of overlying water at rate  $E\bar{u}$  per unit area and the supply of cold water from plumes convecting from the surface at a rate  $\bar{w}F \cos \beta$  per unit area of the sloping bottom, where  $F$  is the fraction of the area covered by vertical plumes. The volume conservation equation can therefore be written as

$$\frac{d(\bar{u}h)}{dx} = E\bar{u} + \bar{w}F \cos \beta \quad (1)$$

Horizontal sections made by a submarine in the convective upper layer at about 10 m depth show convecting plumes to be about 5 m across with a mean separation of 17 m between the centers of adjacent events (see Thorpe et al. 1999 for details). Assuming that the plumes are circular in shape, their radius can be estimated to be  $2\pi^{-1}$  times the observed extent covered by the submarine or  $10\pi^{-1}$  m. The plume area per unit horizontal area is therefore  $F = [\pi(10\pi^{-1})^2]17^{-2} = 0.11$ .

In the steady state, the balance between the driving buoyancy force and the drag can be written

$$\begin{aligned} g'h \sin \beta - \frac{1}{2} \frac{d(g'h^2 \cos \beta)}{dx} + (\bar{w}F \cos \beta)(\bar{w}F \sin \beta) \\ = C_D \bar{u} \sqrt{\bar{u}^2 + \bar{v}^2} \end{aligned} \quad (2)$$

Here it is again assumed that  $\bar{u} \gg \bar{w} \sin \beta$ . The terms on the left-hand side of Eq. 2 are the driving buoyancy force, the pressure force on the gravity current due to its changing thickness, and the momentum input from the plumes, respectively. The term on the right-hand side is the turbulent frictional drag with drag coefficient,  $C_D$ , taken to include both the effects of friction on the slope and the interface between the gravity current and the ambient water. The reduced acceleration of gravity,  $g'$ , in the gravity current can be written as  $g\alpha(\theta_{\text{amb}} - \theta)$  in the freshwater Lake Geneva because the density only changes with variations in temperature. Here,  $\alpha$  is the thermal expansion coefficient of fresh water, typically  $4.6 \times 10^{-5} \text{C}^{-1}$  at  $7^\circ\text{C}$ .

The conservation of heat in the gravity current implies that

$$\bar{u}h \frac{\partial \theta}{\partial x} = E\bar{u}(\theta_{\text{amb}} - \theta) - \bar{w}F \cos \beta (\theta - \theta_p) \quad (3)$$

The terms on the right-hand side of Eq. 3 indicate the heat input from the relatively warmer ambient water due to entrainment and the heat loss as a consequence of the cold vertical plume.

*Results and discussion*—The mean cycle of the cascade and the analysis of individual slugs show that the volume flux in the gravity current as well as its thickness increase with downslope distance (Fer et al. 2001). Twenty-five individual slugs of cold water, which were successfully followed between the two consecutive moorings at 21 and 55 m depth, are analyzed to estimate  $C_D$  and the relative contributions of entrainment and the convective vertical plumes.

The cold slug shown in Fig. 2 is one of the 25 events recorded during the period of observation. It is first recorded by the vertical array 21 m depth (Fig. 2a) at 0600 h local time on 14 January 2000. The downslope current,  $u$ , recorded by the ACMs at 2 and 4 m above the bottom at the same location increases as the slug passes (Fig. 2b). The slug is observed to arrive later, at 0900 h, at the vertical array 55 m depth (Fig. 2c). The ADCP record (Fig. 2d) shows that the downslope flow associated with the slug exceeds  $5 \text{ cm s}^{-1}$ .

At 21 m, the thickness of the gravity current,  $h$ , is estimated as that of the bottom layer in which the temperature  $\theta$  is lower than the ambient temperature  $\theta_{\text{amb}}$ , calculated as the mean temperature recorded by the topmost sensors of both vertical arrays, over the 30-min period before the slug starts. Because the vertical thermistor array at 55 m depth is too short for such estimates,  $h$  is taken as the height where the downslope speed,  $u$ , recorded by the ADCP was zero. In Fig. 3, a CTD profile taken on 14 January 2000 at about 1235 h local time is compared to the mean downslope velocity profile averaged over the duration of the slug between 9 and 12 h (see Fig. 2c–d). The CTD profiling depth is 50 m. The apparent thickness

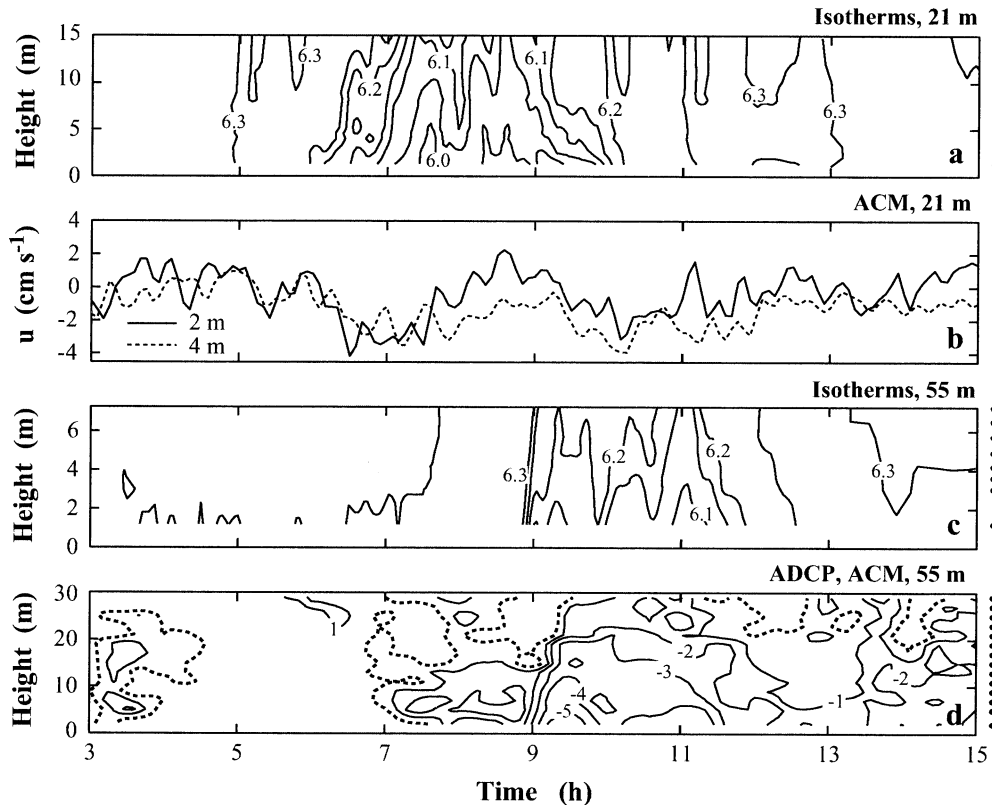


Fig. 2. The movement of a slug of cold water down the slope recorded on 14 January 2000. Time is local time and height is given above the bottom. The dots on the right of (a) and (c) indicate the height of deployed thermistor miniloggers, whereas those on (d) show the location of the ACM 2 m above the bottom and the 2-m bins of the ADCP. Contour intervals for temperature and speed are  $0.05^{\circ}\text{C}$  and  $1 \text{ cm s}^{-1}$ , respectively. The data presented are smoothed over 10 min. (a) Isotherms derived from the vertical array at 21-m show a slug of cold water between 0600 and 1100 h. (b) The upslope component of current measured by the ACMs at 2 and 4 m above the bottom. Negative values indicate downslope movement. (c) Temperature contours derived from the vertical array at 55 m depth. The slug arrives at about 0900 h and persists for approximately 3 h. (d) Contours of upslope current component measured by the bottom-mounted ADCP and the ACM at 55 m depth. The ACM is 2 m above the bottom and ADCP starts profiling at 5 m above the bottom with 2-m bins. The dashed contour is  $u = 0 \text{ cm s}^{-1}$ .

of the cold bottom layer in the temperature profile agrees well with the thickness of the region of downslope flow ( $u < 0 \text{ cm s}^{-1}$ ). This suggests that  $h$  can be estimated from the  $u$  profile with some confidence.

At 21 m depth, the downslope flow,  $u$ , recorded by the 2-m off-bottom current meter is used, whereas at 55 m depth, a vertical profile of  $u$  is obtained from the ADCP data. Making use of the measured time series of  $u$  and  $\theta$  and the estimated values of  $h$  and  $\theta_{\text{amb}}$ , the buoyancy flux,  $B_s$ , and the volume flux,  $q$ , of the gravity current per unit alongslope length are estimated using

$$B_s = g\alpha \int_T \int_0^{z_{\text{at } u=0}} (\theta_{\text{amb}} - \theta) u \, dz \, dt \quad \text{and} \quad (4)$$

$$q = \frac{1}{T} \int_T \int_0^{z_{\text{at } u=0}} u \, dz \, dt \quad (5)$$

Here,  $T$  is the total duration of an observed slug of cold

water and  $z$  is the vertical distance normal to the slope. In Eqs. 4, 5, the upper limit of integration with respect to  $z$  is set to the height above the bottom where  $\theta = \theta_{\text{amb}}$  for the calculations at 21 m depth. The mean downslope flow,  $\bar{u}$ , at corresponding moorings is estimated by averaging the downslope component of the current, recorded 2 m above the bottom by the Aanderaa current meters, over the duration of each slug. Using the uppermost thermistors of the vertical arrays, the vertical plume temperature,  $\theta_p$ , is estimated as the temperature that is lower than that of the slug during the time of its passage. The vertical plume events are episodic and  $\theta_p$  is set to zero when no plume is detected.  $\theta - \theta_p$  is equal to  $0.02 \pm 0.01^{\circ}\text{C}$ , on average ( $\pm 1 \text{ SD}$ ).

The buoyancy flux of the gravity current,  $B_s$ , normalized by the surface buoyancy flux over the shelf integrated from one slug of cold water to the next doubles on average as the gravity current passes from 21 m to the mooring at 55 m.

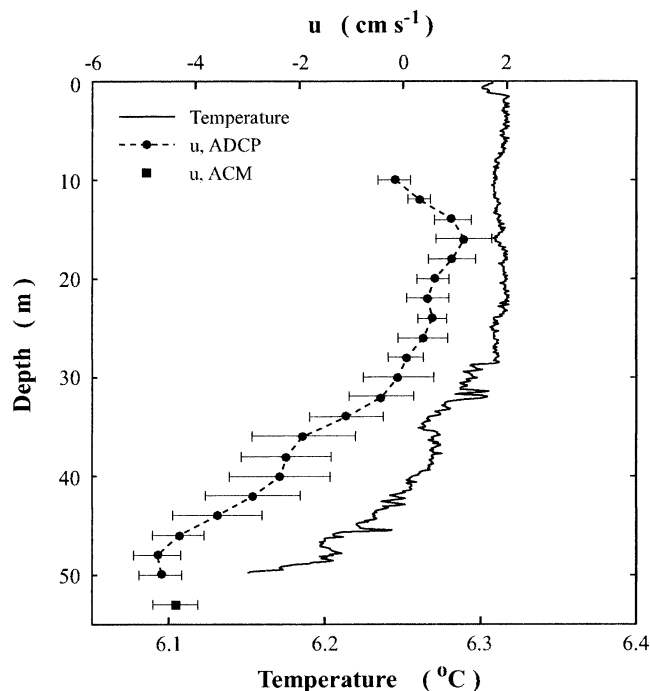


Fig. 3. Profiles of temperature and the upslope component of the current on 14 January 2000. The temperature profile is taken by a CTD instrument at about 1235 h local time. The profiling depth is 50 m. The velocity profile is derived from the ADCP record at 55 m by averaging over the duration of the slug between 0900 and 1200 h. The value corresponding to 2 m above the bottom is recorded by the ACM at the same depth. The bars show one standard deviation of the variability estimated over the duration of the slug. Negative values indicate downslope movement.

The volume in the gravity current,  $V_s$  (i.e., the volume of the entire slug over its duration at the corresponding arrays), is about  $3.7\bar{V}$  at 21 m and increases up to  $11.5\bar{V}$  at 55 m, where  $\bar{V} = \bar{d}l$  is the mean volume of the shelf water in Buchillon, with  $\bar{d} = 4$  m, the average depth to the ‘shelf break’ at about  $l = 400$  m from shore where the bottom slope increases sharply.

The three unknowns— $C_D$ ,  $\bar{w}F$ , and  $E\bar{u}$ —can be calculated using Eqs. 1–3. The variation of  $C_D$  is given in Fig. 4a as a function of  $\bar{d}|L|^{-1}$  where  $L$  is the Monin–Obukov length scale:  $L = -u_*^3/(\kappa B)^{-1}$ . Here,  $\kappa = 0.41$  is the von Karman constant,  $u_*$  is the shear velocity derived from wind, and  $B$  is the surface buoyancy flux.  $B$  and  $u_*$  are estimated from meteorological data recorded from a mast located in the region. Uncertainties in the values of  $B$  and  $L$  are estimated to be 10 and 15%, respectively. On average,  $C_D$  is equal to  $(4.6 \pm 1.5) \times 10^{-3}$ . This is slightly larger than the values given in the literature (e.g.,  $3 \times 10^{-3}$  [Britter and Linden 1980] and  $2.5 \times 10^{-3}$  [Lane-Serff 1993]). The ratio  $E\bar{u}(\bar{w}F)^{-1}$  is shown in Fig. 4b as a function of  $\bar{d}|L|^{-1}$ ;  $E\bar{u}(\bar{w}F)^{-1} = 1.9 \pm 0.9$ . This suggests that the contribution of vertical plumes may be important for the dynamics of the cascade.

The entrainment coefficient,  $E$ , is found to be  $0.03 \pm$

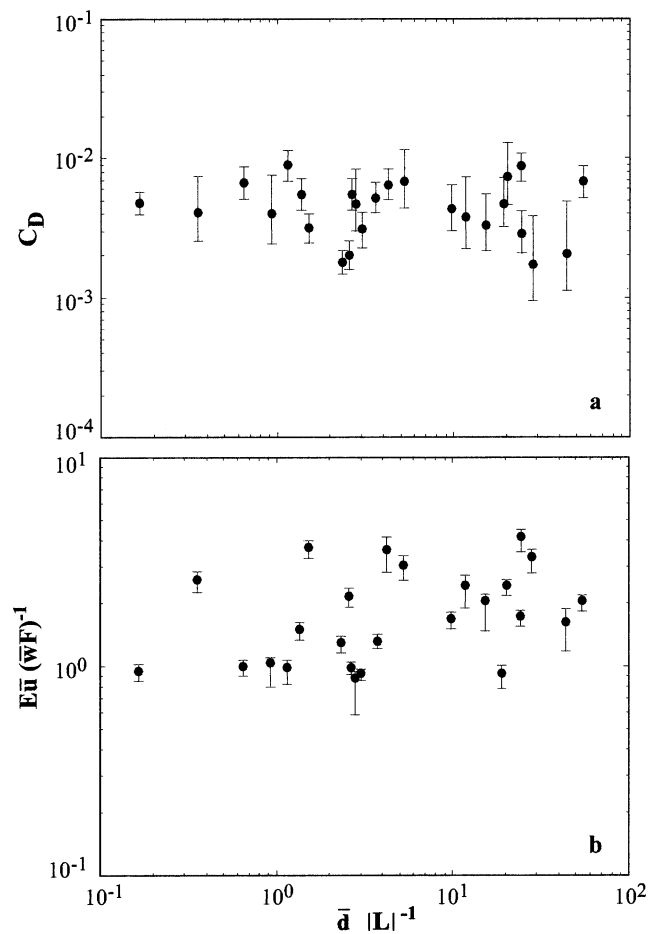


Fig. 4. The variation of (a) the drag coefficient,  $C_D$ , and (b) the ratio of the volume per unit area of the sloping bottom entrained into the slug,  $E\bar{u}$ , and that supplied by the vertical plumes,  $\bar{w}F$ , with respect to  $\bar{d}|L|^{-1}$ .  $\bar{d} = 4$  m is the mean shelf depth, and  $L$  is the Monin–Obukov length. The error bars are estimated from the uncertainties in  $\bar{u}$ ,  $h$ , and temperature.

0.01. Introducing typical values of  $\bar{u} = 5$  cm s $^{-1}$  and  $F = 0.11$ , an estimate of  $\bar{w} = 0.7 \pm 0.2$  cm s $^{-1}$  can be obtained. The downslope component of the flow induced by the convecting plumes,  $\bar{w} \sin \beta$ , can then be calculated as  $0.06 \pm 0.02$  cm s $^{-1}$ , which is far lower than  $\bar{u}$ . Therefore, our assumption that  $\bar{u} \gg \bar{w} \sin \beta$  is applicable. The dependence of the entrainment coefficient on the overall Richardson number,  $Ri_o = g'h \cos \beta \bar{u}^{-2}$ , as a function of  $E(Ri_o)$  was proposed by Ellison and Turner (1959) and can be approximated by  $E = (0.08 - 0.1Ri_o)(1 + 5Ri_o)^{-1}$  (Turner 1986). Using the typical values of  $h \approx 15$  m,  $\bar{u} \approx 5$  cm s $^{-1}$ , and  $(\theta_{amb} - \theta) \approx 0.1^\circ\text{C}$ ,  $Ri_o \approx 0.27$  is obtained. This yields an entrainment coefficient of  $E \approx 0.02$ , which compares well with our calculations.

The simple model used here describes the early stages of flow and indicates the relative importance of processes. Turbulent entrainment provides heat input into the gravity current while vertical plumes penetrating into it add colder water masses, thus enhancing downslope motion. It is observed that a mean cyclonic alongslope flow,  $\bar{v}$ , develops within a

few hours of the commencement of a cold downslope flow (Fer et al. 2001), and over longer times and greater depth, the effects of the Earth's rotation may become important. However, this will not significantly affect the result we obtained from the analysis above.

*Ilker Fer<sup>1</sup> and Ulrich Lemmin*

Laboratoire de Recherches Hydrauliques  
Dépt. Génie Civil  
Ecole Polytechnique Fédérale de Lausanne  
CH-1015 Lausanne, Switzerland

*S. A. Thorpe*

School of Ocean and Earth Science  
Southampton Oceanography Centre  
European Way  
Southampton SO14 3ZH, United Kingdom

### References

- BRITTER, R. E., AND P. F. LINDEN. 1980. The motion of the front of a gravity current travelling down an incline. *J. Fluid Mech.* **99**: 531–543.
- COOPER, L. H. N., AND D. VAUX. 1949. Cascading over the continental slope of water from the Celtic Sea. *J. Mar. Biol. Assoc. UK* **28**: 719–750.
- CRAWFORD, G. B., AND R. W. COLLIER. 1997. Observation of a deep mixing event in Crater Lake, Oregon. *Limnol. Oceanogr.* **42**: 299–306.
- ELLISON, T. H., AND J. S. TURNER. 1959. Turbulent entrainment in stratified flows. *J. Fluid Mech.* **6**: 423–448.
- FER, I., U. LEMMIN, AND S. A. THORPE. 2001. Cascading of water down the sloping sides of a deep lake in winter. *Geophys. Res. Lett.* **28**: 2093–2096.
- HILL, A. E., A. J. SOUZA, K. JONES, J. H. SIMPSON, G. I. SHAPIRO, R. MCCANDLISS, H. WATSON, AND J. LEFTLEY. 1988. The Malin cascade in winter. *J. Mar. Res.* **56**: 87–116.
- HUTHNANCE, J. M. 1995. Circulation, exchange and water masses at the ocean margin: The role of physical processes at the shelf edge. *Prog. Oceanogr.* **35**: 353–431.
- KILLWORTH, P. D. 1979. On 'chimney' formation in the ocean. *J. Phys. Oceanogr.* **9**: 531–554.
- LANE-SERFF, G. F. 1993. On drag-limited gravity currents. *Deep-Sea Res. I* **40**: 1699–1702.
- MARSHALL, J., AND F. SCHOTT. 1999. Open-ocean convection: observations, theory, and models. *Rev. Geophys.* **37**: 1–64.
- MCMANUS, J., R. W. COLLIER, J. DYMOND, C. G. WHEAT, AND G. LARSON. 1996. Spatial and temporal distribution of dissolved oxygen in Crater Lake, Oregon. *Limnol. Oceanogr.* **41**: 722–731.
- THORPE, S. A., U. LEMMIN, C. PERRINJAQUET, AND I. FER. 1999. Observations of the thermal structure of a lake using a submarine. *Limnol. Oceanogr.* **44**: 1575–1582.
- TOMCZAK, M. 1985. The Bass Strait water cascade during winter 1981. *Continental Shelf Res.* **4**: 255–278.
- TURNER, J. S. 1973. Buoyancy effects in fluids. Cambridge Univ. Press.
- . 1986. Turbulent entrainment: The development of the entrainment assumption, and its application to geophysical flows. *J. Fluid Mech.* **173**: 431–471.

<sup>1</sup> To whom correspondence should be addressed. Present address: Geophysical Institute, University of Bergen, Allegaten 70, N-5007, Bergen, Norway.

### Acknowledgments

The financial support for this study was provided by the Swiss National Science Foundation, grant 20-49502.96. The constructive comments of the anonymous reviewers and their assistance in evaluating the paper are appreciated.

*Received: 14 May 2001  
Accepted: 29 October 2001  
Amended: 7 November 2001*

## Interpreting stable isotopes from macroinvertebrate foodwebs in saline wetlands

**Abstract**—We compared stable-isotope ( $\delta^{13}\text{C}$  and  $\delta^{15}\text{N}$ ) and gut-content analyses of macroinvertebrate foodwebs in saline wetlands of the Laramie Basin, Wyoming, USA. Standard assumptions of stable-isotope fractionation between trophic levels ( $<1\text{‰}$  for  $\delta^{13}\text{C}$ , mean of  $3.4\text{‰}$  for  $\delta^{15}\text{N}$ ) suggested that zygopteran (damselfly) larvae consumed mainly amphipods. However, the guts of zygopterans contained no amphipods but rather a mix of chironomid larvae and zooplankton. In all wetlands the gut contents of zygopterans indicated that they were secondary consumers (trophic level 3), but enrichment of  $\delta^{15}\text{N}$  between zygopterans and their prey ( $\Delta\delta^{15}\text{N}$ ) varied from 1 to  $3.4\text{‰}$  between wetlands. In other studies, such variation in  $\Delta\delta^{15}\text{N}$  has been interpreted to mean that food-chain length differed between aquatic systems. We review alternative interpretations of variable  $^{15}\text{N}$  enrichment, namely, varying C:N ratios in food, differential enrichment between consumer species, and habitat-specific variation of  $\delta^{15}\text{N}$  at the base of foodwebs. We also suggest that variation in the timing and rates

of nitrogen cycling can affect measured  $\Delta\delta^{15}\text{N}$  both within and between foodwebs. For aquatic macroinvertebrates, we urge that stable isotopes be supplemented with independent observations to avoid incorrect conclusions about trophic pathways, trophic levels, and food-chain lengths in different ecosystems.

Macroinvertebrate foodwebs are the main link between high primary production and top consumers in wetlands. Two main tools for characterizing such foodwebs are gut-content analysis and stable isotopes. The latter method is often used, but there can be problems interpreting stable-isotope data. For example,  $\delta^{13}\text{C}$  typically increases by  $<1\text{‰}$  with each trophic transfer, so that  $\delta^{13}\text{C}$  can be used to discriminate diets derived from different sources of primary production (Peterson and Fry 1987). However, consuming a